Nucleation of weak stripe domains: Determination of exchange and anisotropy thermal variation

G. Asti, M. Ghidini, M. Mulazzi,* R. Pellicelli, and M. Solzi
CNISM and Dipartimento di Fisica, Università di Parma, Viale G. P. Usberti 7/A, 43100 Parma, Italy

K. Chesnel
Advanced Light Source Division, Lawrence Berkeley National Laboratory, Berkeley, California 94720-8226, USA

A. Marty
Département de Recherche Fondamentale sur la Matière Condensée, CEA Grenoble, 17 Avenue des Martyrs, 38054 Grenoble Cedex 9, France

(Received 8 May 2007; revised manuscript received 16 June 2007; published 24 September 2007)

The phenomenon of stripe domain nucleation is deeply investigated both theoretically and experimentally in FePd films by the rigorous micromagnetic theory of domain nucleation and x-ray resonant magnetic scattering. The critical domain width and the nucleation field are determined by measuring the magnetic satellite peak position and integrated intensities in a wide temperature interval up to 400 °C ($0.9T_c$) at varying in-plane magnetic fields for each temperature value. We develop and demonstrate a procedure that allows us to determine directly from the micromagnetic treatment the exchange stiffness constant A and the first order anisotropy constant K_u as a function of temperature. The proposed procedure, based on linearized micromagnetic equations at the critical field, is valid for magnetic films with perpendicular magnetic anisotropy, and is therefore effective to measure A and K_u in a technologically relevant class of materials.

DOI: 10.1103/PhysRevB.76.094414 PACS number(s): 75.70.Kw, 75.60.Ej, 75.60.Ch, 78.70.Ck

I. INTRODUCTION

In this paper, we give a detailed account of a general procedure for determining the thermal variation of the exchange stiffness A and of the first order uniaxial magnetocrystalline anisotropy constant K_u in a technologically relevant class of materials: magnetic films with perpendicular magnetic anisotropy (PMA). In practice, very few methods can be employed to measure A and they are applicable only in special cases, in particular, making use of spin-wave resonance experiments.[1] Static measurements are sometimes utilized to deduce A indirectly from the Curie temperature or from the temperature dependence of the magnetization, in the frame of either molecular field or spin-wave theories.[2] Regarding the temperature dependence of A, little information has been published. In metallic films the few experimental points obtained from spin-wave resonance experiments[3] yield A proportional to M_s^2. In magnetic oxides, the only published data date back to Gemperle *et al.*[4] who studied the domain structure temperature dependence in magnetoplumbite, and subsequently deduced the thermal dependence of A. At intermediate temperature they also observe A to vary as the square of the magnetization. To the best of our knowledge, this remains the only confirmation of the invoked thermal dependence of A as deduced from the relation including the magnetization of the different sublattices.[5]

In the past decade, magnetic films with PMA have attracted renewed interest, mainly for perpendicular magnetic recording, magneto-optic recording, and patterned media. Particular emphasis has been given to films made of intermetallic compounds, such as Fe-Pt, Fe-Pd, and Co-Pt, which crystallize in the tetragonal structure $L1_0$ [CuAu(I) type]. This ordered structure consists of alternating planes of Fe (or Co) and Pt (or Pd) so that the conventional cell has only one fourfold symmetry axis, which is an easy magnetization axis. First order uniaxial anisotropy constants K_u in the range of 10^6-10^7 J/m^3 are reported.[6–8] From the point of view of micromagnetism and magnetization processes, highly pure and ordered layers with a perpendicular easy axis share a common phenomenology. In properly oriented layers, the high K_u can overcome the demagnetizing field of the film, so that the stable magnetization direction lies perpendicularly to the film plane. This situation corresponds to the condition $Q>1$ having introduced the so called quality factor $Q=K_u/K_d$ where $K_d=\mu_0 M_s^2/2$ is the shape anisotropy constant. Films with effective PMA ($Q>1$) are suitable media for high density magnetic recording.[9] Finally, it is worth mentioning also that the recently proposed thermal assisted perpendicular recording is being actively investigated and relies on high K_u perpendicular layers (FePt, in particular).[10,11]

The procedure we propose to determine A and K_u is based on the rigorous treatment of weak stripe domain nucleation with in-plane magnetic field. Although the micromagnetic theory of this process dates back to Muller[12] and Brown,[13] it is worth noting that it has never been applied to PMA films. The search for periodic solutions to the linearized micromagnetic equations at the critical field leads to the construction of phase diagrams in terms of generic reduced variables which can be applied to any material. This feature allows us to measure directly from the micromagnetic equations the intrinsic material parameters A and K_u. The procedure requires two experimentally determined sets of data: the temperature dependence of the stripe domain nucleation field and of the critical domain width. The thermal variation of the spontaneous magnetization M_s must also be known.

For demonstrating the method we select epitaxial films of the tetragonal FePd equiatomic compound. In such systems, above a critical thickness, regular weak stripe domain patterns are formed due to the competition between the magnetocrystalline anisotropy and the shape anisotropy.[14] We de-

termine the thermal variation of both A and K_u up to 400 °C, i.e., almost up to the Curie temperature (about 450 °C). We use x-ray resonant magnetic scattering (XRMS) experiments at different temperatures in variable magnetic fields to measure the temperature dependence of the crucial parameters of the magnetic domain structure. XRMS has the capability of probing striped domain structures,[15] since the regular domain pattern gives rise to magnetic satellite peaks on the specular reflection peak sides, whose position is directly correlated to the domain width W. Although the high spatial resolution achievable with this technique is important in samples showing nanoscale domain patterns, however, our approach does not depend on the particular method chosen to fully characterize the domain structure.

The phenomenon of weak stripe domain nucleation with in-plane magnetic field, as already pointed out by Brown,[13] allows us to access the intrinsic values of the nucleation field and of the critical domain width, since the role of imperfections should be negligible. It is known that the influence of defects is of paramount importance in the magnetization reversal of a ferromagnet. Indeed, reversal at the switching field is an irreversible process initiated locally at a defect, implying a transition from a metastable state to the stable state at a negative internal field. Even a small number of defects representing the "weak point" of the system, determines the magnetic reversal. In the present case, we deal with a different situation, in which the domain nucleation is a collective phenomenon described by a continuous reversible process of the magnetic system always at its absolute energy minimum. The presence of diluted defects only implies a negligible and continuous alteration of the total energy of the system which is reflected in a negligible modification of the overall demagnetization process. Moreover, the adopted experimental procedure, based on a magnetic diffraction technique, inherently provides evidence of the specific global character of the transition we observe: the presence of a periodic configuration of the gradually emerging domain structure. A localized defect or a random distribution of imperfections could hardly establish at a precise critical field such a regular and spatially extended pattern.

Our procedure allows one to determine the thermal dependence of A and of K_u in PMA films. Recently, the thermal dependence of K_u has been predicted to follow M_s^2 in FePd (Ref. 16) and FePt (Ref. 17) on the basis of relativistic calculations of electronic properties. Then, in these materials one should expect a constant A/K_u ratio when temperature is varied. This fact would yield a stripe domain structure with a distinctive feature, namely, that the representative point in the phase diagrams does not vary.

II. EXCHANGE STIFFNESS AND ANISOTROPY FROM STRIPE DOMAIN NUCLEATION

Let us consider an infinite slab of thickness D along y axis under the action of a uniform external field, H, in the plane of the slab, parallel to z axis (Fig. 1). Starting from saturation, we reduce H until a critical condition is realized at a value $H=H_c$ at which the magnetization vector starts to deviate from the z direction, giving rise to weak stripe domains

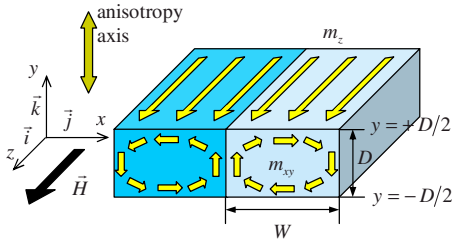

FIG. 1. (Color online) Basic scheme for the weak stripe domain micromagnetic model of the film with anisotropy axis perpendicular to the film plane and the external field applied in the film plane.

parallel to the field direction. The theory of weak stripe domain nucleation allows calculation of the critical field H_c and the critical domain width W_c at nucleation if the intrinsic material parameters A, K_u, and M_s, and the thickness D of the sample are known. Conversely, if W_c, H_c, and M_s are known experimentally, the A and K_u values can be deduced.

In fact, we have carried out an in-depth analysis of the theory, in order to formulate all the equations in a suitable manner to be easily compared with the experimental data. In this section a brief overview of our theoretical treatment is given. A detailed description is reported in the Appendix, since the mathematical treatment is an essential part of the overall measurement procedure. The magnetization equilibrium condition inside a single homogeneous film with perpendicular anisotropy is

$$\vec{m} \times \vec{H}_{\text{eff}} = \vec{m} \times [(2A/\mu_0 M_s)\nabla^2 \vec{m} + (2K_u/\mu_0 M_s) \times m_y \vec{j} - \vec{\nabla}\Phi + H\vec{k}] = 0, \quad (1)$$

where $\vec{m}$ is the magnetization unit vector, Φ is the scalar potential of the magnetostatic field, and $\vec{H}_{\text{eff}}$ is the total effective field, obtained as the sum of exchange, anisotropy, magnetostatic, and external fields. The following dimensionless quantities can be conveniently introduced:

$$\xi = \frac{x}{a}, \quad \eta = \frac{y}{a}, \quad \zeta = \frac{z}{a}, \quad \delta = \frac{D}{a}, \quad \varphi = \frac{\Phi}{aM_s}; \quad (2)$$

$$\vec{h} = \frac{\vec{H}}{H_K}; \quad \vec{h}_{\text{eff}} = \frac{\vec{H}_{\text{eff}}}{H_K},$$

where $H_k = 2K_u/\mu_0 M_s$ and $a = \sqrt{A/K_u}$. Equation (1) becomes $\vec{m} \times \vec{h}_{\text{eff}} = 0$ with

$$\vec{h}_{\text{eff}} = \nabla^2 \vec{m} + m_y \vec{j} - \frac{1}{Q}\vec{\nabla}\varphi + h\vec{k},$$

where $\vec{\nabla}$ is now the gradient operator with respect to ξ, η, and ζ. Considering that at nucleation $m_x, m_y \to 0$ and $m_z \cong 1$ to first order, the vectorial equilibrium condition (1) reduces to only two differential equations which must be solved simultaneously with the one relating the potential to the magnetic charges as follows:

$$\nabla^2 m_y + (1-h)m_y - \frac{1}{Q}\frac{\partial \varphi}{\partial \eta} = 0,$$

$$\nabla^2 m_x - m_x h - \frac{1}{Q}\frac{\partial \varphi}{\partial \xi} = 0,$$

$$\frac{\partial m_x}{\partial \xi} + \frac{\partial m_y}{\partial \eta} - \nabla^2 \varphi = 0. \tag{3}$$

The scalar potential outside the film, $\tilde{\varphi}$, satisfies the Laplace equation

$$\nabla^2 \tilde{\varphi} = 0. \tag{4}$$

The boundary conditions at the film surfaces are

$$\left.\frac{\partial m_x}{\partial \eta}\right|_{\eta=\pm\delta/2} = \left.\frac{\partial m_y}{\partial \eta}\right|_{\eta=\pm\delta/2} = 0, \tag{5}$$

$$\tilde{\varphi}|_{\eta=\pm\delta/2} = \varphi|_{\eta=\pm\delta/2},$$

$$\left.\frac{\partial \tilde{\varphi}}{\partial \eta}\right|_{\eta=\pm\delta/2} - \left.\frac{\partial \varphi}{\partial \eta}\right|_{\eta=\pm\delta/2} = -m_y|_{\eta=\pm\delta/2},$$

while at infinity it must be

$$m_x|_{\xi,\zeta=\pm\infty} < \infty, \quad m_y|_{\xi,\zeta=\pm\infty} < \infty, \quad \varphi|_{\xi,\zeta=\pm\infty} < \infty, \tag{6}$$

$$\tilde{\varphi}|_{\xi,\zeta=\pm\infty} < \infty, \quad \tilde{\varphi}|_{\eta=\pm\infty} = 0.$$

A class of solutions is represented by periodic functions of the form

$$(m_x, m_y, \varphi) = (B, C, U)e^{i(\alpha\xi+\beta\eta+\gamma\zeta)}, \quad (\tilde{m}_x, \tilde{m}_y, \tilde{\varphi})$$
$$= (0, 0, \tilde{U})e^{i(\tilde{\alpha}\xi+\tilde{\beta}\eta+\tilde{\gamma}\zeta)}. \tag{7}$$

Substituting the ansatz (7) in Eqs. (3)–(5), an algebraic linear system of equations is obtained. The existence of nontrivial solutions representing nucleation of the stripe domain structure requires that the determinant of the coefficient matrix is vanishing. This yields a secular equation for α, γ [the reduced wave vectors introduced in Eq. (7)], and δ and h [defined in Eq. (2)]. The energy minimization implies that nucleation takes place for the reduced wave numbers α and γ in correspondence to which δ is minimum at fixed h (these critical values are symbolized with δ_c and h_c in Fig. 2). It can be demonstrated that for $\alpha^2+\gamma^2$ comprised between zero and $1-h_c$, there exists certainly a minimum δ_c for δ.[18] The numerical calculations show that the solution of minimum energy can be always found with two-dimensional functions independent of z ($\gamma=0$). As a consequence, the stripe domain pattern is parallel to the external field, and the reduced domain width, defined as half-period $w=W/a$, is related to the reduced wave number α along the x direction ($w=\pi/\alpha$). On the other hand, this two-dimensional configuration is typically observed in the experimental conditions. The results of this analysis are well synthesized in the universal curves of the phase diagrams giving the critical parameters of the domain structure nucleation in terms of the intrinsic material properties (see Fig. 2). From the comparison of these universal curves with specific experimental features, one could obtain accurate determinations of crucial parameters characterizing a particular magnetic material. The implemented procedure is as follows. Experimentally, the nucleation field H_c and the critical domain width W_c have to be measured at different temperatures for a platelet having a known thickness D, which obviously coincides with the critical thickness D_c. Moreover, the thermal dependence of the spontaneous magnetization M_s must be known. For each temperature, we assign to K_u the value which assures agreement in the diagram of Fig. 2(b), between the theoretical and the experimental values of the ratio $D/W_c(=\delta/w_c)$. Afterwards we extract the values of the exchange stiffness A from the expression $A=D^2/\delta^2 K_u$, which follows directly from the definition of δ. It should be noted that the above procedure is particularly versatile since Q, h_c, and δ/w_c do not depend on A, a circumstance which is determined by the suitably chosen set of reduced variables. Figure 2 reports the complete phase diagrams synthesizing all the possible nucleation conditions for any material. In Fig. 2(a) the reduced critical thickness divided by 2π and in Fig. 2(b) the inverse of the critical domain width normalized to the film thickness are reported as a function of the quality factor for different values of the reduced nucleation critical field. In the diagrams, we depict selected isofield lines.

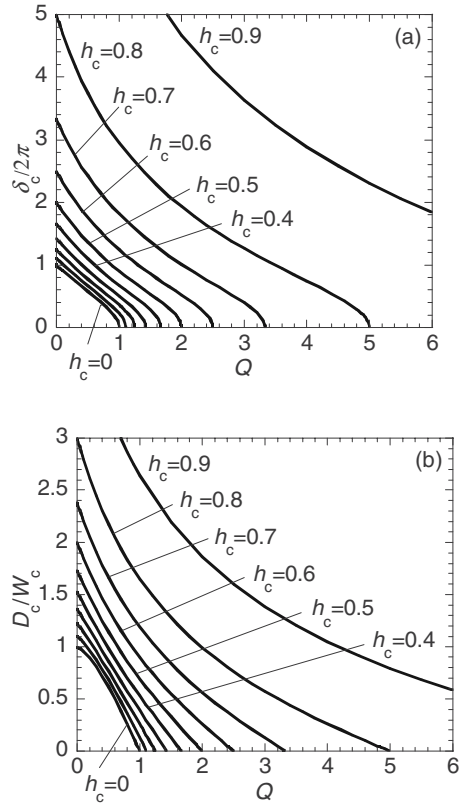

FIG. 2. Calculated phase diagrams for weak stripe domain nucleation. (a) The ratio $\delta_c/2\pi$ is plotted as a function of Q for different values of the reduced critical nucleation field h_c. (b) The ratio D_c/W_c is plotted as a function of Q for different values of the reduced critical nucleation field h_c. Both horizontal and vertical scales are linear.

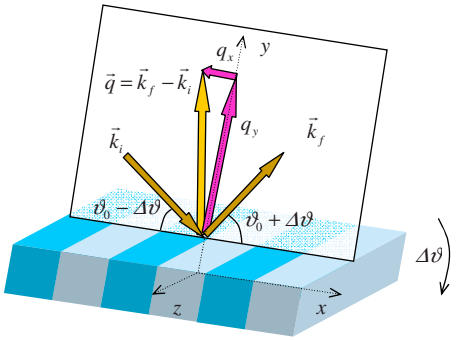

FIG. 3. (Color online) XRMS experimental geometry with x rays incident perpendicularly to the stripe direction at an angle centered at ϑ_0.

It can be readily demonstrated that the coherent rotation is a particular solution [not belonging to the ansatz (7)] of the weak stripe model [see the general equation (1)], with a critical field given by $h_c = h_A = H_A/H_k = 1 - 1/Q < 1$ where $H_A = 2(K_u - K_d)/\mu_0 M_s$ is the overall anisotropy field. As shown by Brown,[13] also the nucleation of noncoherent mode happens always with $h_c < 1$. Being the coherent rotation an overconstrained solution[13] of the micromagnetic equations, then the weak stripe domain nucleation field is $h_c \geqslant h_A$. For weak anisotropy $(Q < 1)h_A$ is negative, so in principle one could obtain from the theory negative values for h_c. However, this is never the case, since the magnetization becomes unstable at the zero-field cross (it undergoes a sudden jump around the y axis toward the reversed saturated state),[19] so that one must assume $h_c \geqslant 0$. For strong anisotropy h_A is definitely positive and coincident with the limit of h_c when $\delta \to 0$ and correspondingly $D/W_c \to 0$. In conclusion, weak stripe domain nucleation has physical meaning when $h_c > 0$ for $Q < 1$ and when $h_c \geqslant h_A = 1 - 1/Q$ for $Q > 1$.

III. EXPERIMENT

An epitaxial FePd film was grown by molecular beam epitaxy on a MgO substrate, with the structure MgO/Cr/Pd/FePd(43 nm)/Pd as described elsewhere.[20,21] The Cr seed layer facilitates the epitaxial growth of the 60 nm Pd single crystal buffer layer. The FePd layer has been deposited at room temperature in a "layer by layer" mode (alternation of Pd and Fe deposition). The 20 nm thick Pd capping layer avoids oxidation. The thickness and crystal structure of the sample were determined by x-ray reflectivity and diffraction, respectively. PMA in FePd films has a bulk origin and is basically independent of the sample thickness, while it depends on the chemical order, and specifically on the stabilization of the $L1_0$ phase. Uniaxial ordering can be controlled during epitaxial growth and the magnetization can be stabilized perpendicularly to the film plane. Vibrating sample magnetometry was used to check the magnetic quality of the sample. XRMS experiments were carried out on the SB7 SuperAco (LURE) beamline at the Fe $L3$ edge ($\lambda = 17.5$ Å). The scanning geometry is sketched in Fig. 3 and the procedure utilized to collect experimental data is

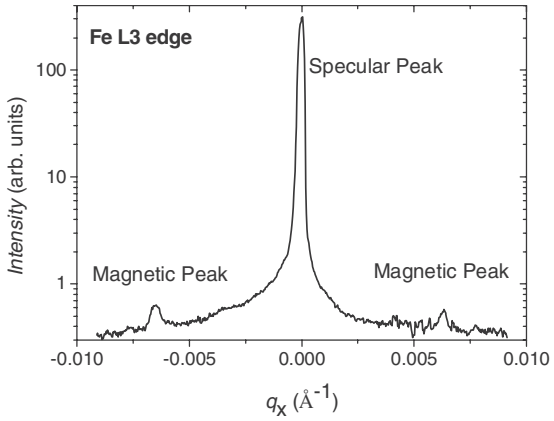

FIG. 4. Diffraction scan with the wave vector q_x transferred along the x axis perpendicular to the magnetic stripes. The beam, whose energy is tuned to the Fe $L3$ edge ($h\nu = 708$ eV), impinges at angle $\vartheta_0 8°$ relative to the film surface.

similar as in Ref. 22. Scans at constant temperatures, from RT up to 400 °C ($0.9T_c$), were performed at different external in-plane magnetic fields. As an example, Fig. 4 reports a typical recorded spectrum. Two magnetic satellite peaks are neatly observed offset by the central specular peak by 0.0065 Å^{-1} corresponding to a real space period (which is twice the average domain width) of 96 nm. In Fig. 5 the typical observed evolution of the magnetic diffraction peak with varying external field is reported corresponding to $T = 125$ °C. It turns out that the integrated intensity of the magnetic signal is increasing with decreasing the applied field below a certain critical value H_c, which can be determined by extrapolation to zero of the satellite peak intensity versus magnetic field. In Fig. 6 the thermal dependence $H_c(T)$ as obtained by iterating the above procedure at different temperatures is reported. The domain width at nucleation W_c was observed to be nearly independent of temperature and determined to have an average value $\langle W_c \rangle = 48.2$ nm, with a varia-

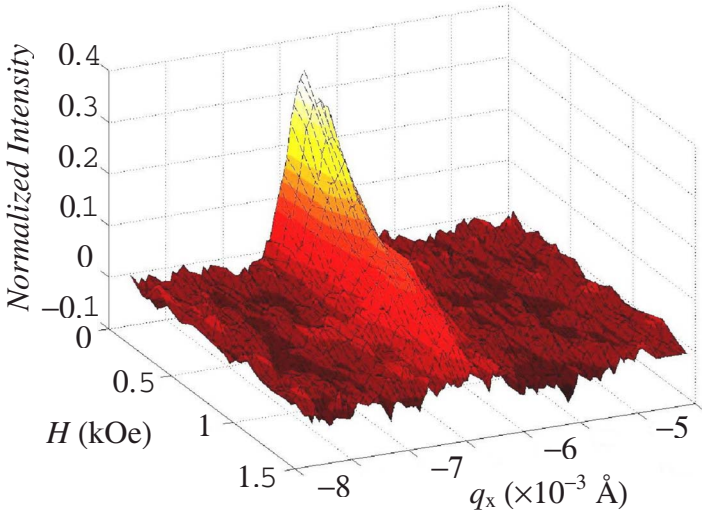

FIG. 5. (Color online) Intensity of the magnetic diffraction peak plotted as a function of q_x and of the external in-plane magnetic field H at constant temperature ($T = 125$ °C).

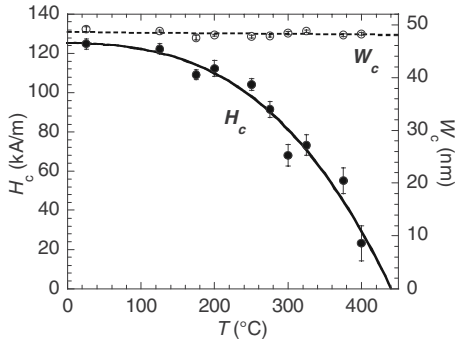

FIG. 6. Critical nucleation field H_c and critical domain width W_c versus temperature as determined from XRMS experiments.

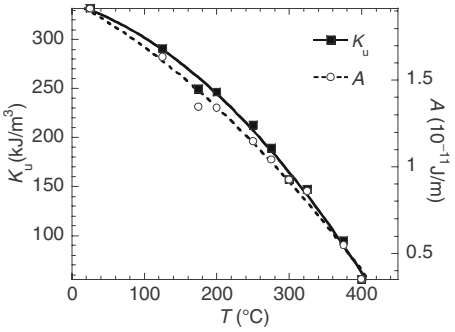

FIG. 7. Exchange stiffness and uniaxial anisotropy constants plotted as a function of the temperature.

tion of ±1 nm over the 25–400 °C interval (Fig. 6). Table I lists all the considered and measured values of T, H_c, and W_c. The M_s values shown in the same table have been obtained from Ref. 6 in the case of equiatomic FePd bulk material. In fact, measuring M_s in thin films in the high temperature range is an extremely difficult task.

IV. DATA ANALYSIS AND DISCUSSION

Applying the procedure described in Sec. II allows us to obtain the values of K_u and A reported in Table I. Figure 7 compares the temperature dependence of K_u and A. They are both observed to decrease monotonically with temperature with a surprising similar behavior over the whole temperature range. In fact, the relation between A and K_u can be fitted by a linear law with a least squares correlation coefficient $R=0.996\,67$ and a relative standard error $\varepsilon=0.01$ (see Fig. 8). Therefore we conclude that the anisotropy and the exchange parameters follow a very similar temperature law within the considered temperature range. This property is a direct consequence of the constancy of the domain width when changing the temperature. Indeed, if we examine the general phase diagrams of Fig. 2, we note that they have a similar pattern. This characteristic implies that if the domain width W_c (and consequently the ratio D_c/W_c; we recall that in our case the critical thickness $D_c=D$ is obviously fixed) is constant, the reduced thickness δ_c and so the ratio A/K_u turn out to be nearly constant. If the dependence of K_u on M_s follows a power law with exponent m, then the variation of Q with M_s is $Q=Q_{\max}(M_s/M_{s,\max})^{m-2}$ where $Q_{\max}$ and $M_{s\max}$ are related to the minimum temperature value. If we suppose that $m>2$, then Q decreases with increasing temperature. The maximum possible variation of Q is equal to $Q_{\max}-Q_{\inf}$, where $Q_{\inf}$ is a lowest limit that can be deduced from Fig. 2(b) ($Q_{\inf}$ is zero if $D_c/W_c>1$, otherwise it is >0). Figure 9 shows the calculated curves $\delta_c/2\pi$ and A/K_u as a function of Q, corresponding to the fixed value $D_c/\langle W_c\rangle=0.892$. The variation of A/K_u in the interval from $Q_{\inf}$ to $Q_{\max}$ is ±10%, a result which does not depend on the true behavior of M_s when the temperature T is varied. In the present experiment the actual variation of Q is smaller and correspondingly A/K_u changes even less. In the extreme hypothesis of assuming both A and K_u proportional to M_s^2, the quantities h_c and Q would remain perfectly constant with temperature, so the representative critical point would maintain fixed positions in the phase diagrams, yielding constant δ_c and W_c. Indeed, our results provide representative points

TABLE I. Summary of all the relevant physical parameters as measured and calculated in the analysis of the XRMS experiment: the temperature T, the nucleation field H_c, the nucleation domain width W_c, the uniaxial magnetocrystalline anisotropy constant K_u, the exchange constant A, the quality factor Q, and the reduced nucleation field h_c. The values of the saturation magnetization M_s are extracted from Ref. 6.

T (°C)	H_c (kA/m)	W_c (nm)	M_s (MA/m)	K_u (kJ/m^3)	A (J/m$\times 10^{-11}$)	Q	h_c
25	124.86	49.16	1.092	331.63	1.91	0.443	0.258
125	122.27	48.78	1.018	290.78	1.63	0.447	0.269
175	109.14	47.55	0.972	249.96	1.35	0.421	0.267
200	112.32	48.02	0.949	246.38	1.34	0.435	0.272
250	104.17	47.76	0.886	212.71	1.15	0.431	0.273
275	91.47	47.88	0.848	189.04	1.04	0.418	0.258
300	68.00	48.40	0.803	157.64	0.92	0.389	0.218
325	73.33	48.78	0.753	147.24	0.86	0.413	0.236
375	55.11	48.04	0.623	95.26	0.55	0.391	0.226
400	23.20	48.27	0.528	55.44	0.35	0.316	0.139

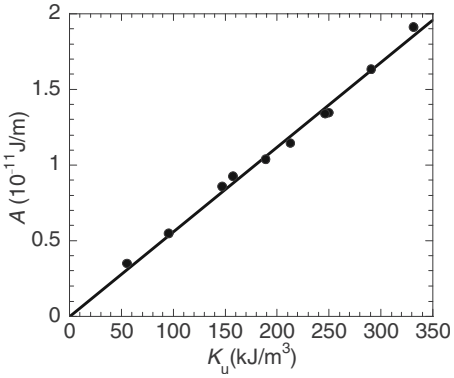

FIG. 8. Linear fit of the experimental exchange constant as a function of the experimental uniaxial anisotropy constant.

at different temperatures falling in a small interval of δ_c and W_c in correspondence to a relatively small variation of Q (see Table I and Fig. 10).

Actually, from our procedure we obtain a dependence of K_u on M_s which can be fitted by a power law with exponent $m=2.4$ and correlation coefficient $R=0.997\,64$ [see Fig. 11(a)]. The direct fitting of the dependence of A on M_s yields a power law with exponent $m=2.25$ and correlation coefficient $R=0.995\,96$ [see Fig. 11(b)]. However, a wide region of low M_s values is not supported by the experimental data. The lack of data is a consequence of the chosen experimental parameters. In any case, the nucleation phenomenon for small values of M_s would not be guaranteed to occur for the assumed film thickness (see Fig. 2). If we take into account that the deduced m exponent values depend critically on the assumed M_s versus T dependence (we remember that we have adopted the M_s values of equiatomic FePd bulk material as given in Ref. 6), the uncertainty is such that our results are substantially in agreement with the data reported in literature which give A varying as M_s^2, as already reported for metallic films.[3,4] The room temperature value of $A=1.91\times10^{-11}$ J/m is slightly lower than the value for Fe (Ref. 23) and significantly higher than the value reported for FePt films by Okamoto *et al.*[24] On the other hand, our value for FePd agrees reasonably with the value calculated by Belashchenko[25] for the in-plane components of tensor A_{ik}.

Concerning the anisotropy constant K_u, the value obtained at room temperature is perfectly compatible with the data

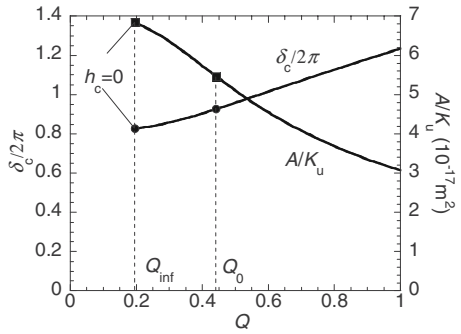

FIG. 9. Theoretically calculated dependence of $\delta_c/2\pi$ and A/K_u on Q with fixed $D_c/W_c=D_c/\langle W_c\rangle=0.892$.

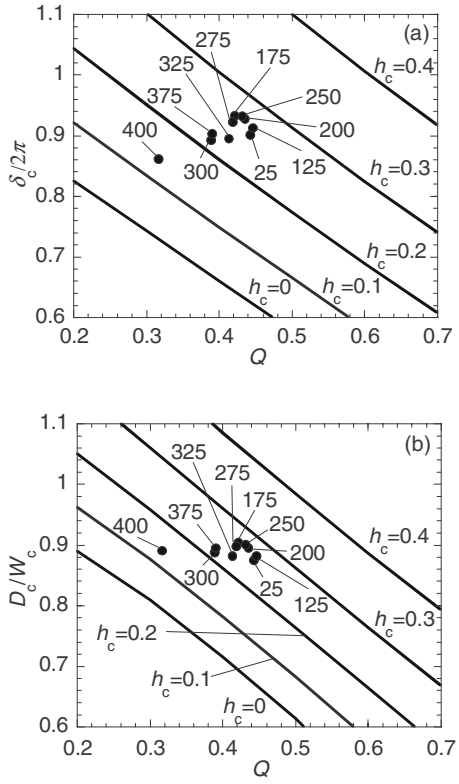

FIG. 10. Evolution of the representative point of the system in the phase diagrams at different considered temperatures.

reported in the literature for FePd films with weak anisotropy.[20] As for the K_u variation with M_s, we point out that the found exponent 2.4 depends on the specific utilized values of M_s, so any conclusive argument should be taken cautiously since we do not dispose of true experimental data concerning our film. A recent paper by Staunton *et al.*[16] developed a first-principles theory based on relativistic electronic structure theory, of the variation of magnetic anisotropy K_u with temperature in metallic ferromagnets. They applied the theory to a uniaxial magnetic material with tetragonal crystal symmetry, $L1_0$-ordered FePd, with easy axis perpendicular to the Fe/Pd layers. To our knowledge this is the only attempt to evaluate the magnetic anisotropy variation up to the Curie temperature. Their theory predicts for FePd a M_s^2 dependence of K_u. The same result was previously found also in $L1_0$-ordered FePt.[17]

V. CONCLUSIONS

We have successfully demonstrated a method to measure directly from the micromagnetic equations the intrinsic materials parameters A and K_u in films with PMA. The procedure is based on the rigorous treatment of weak stripe domain nucleation with in-plane magnetic field. Using high temperatures XRMS measurements in varying magnetic fields, we have been able to determine the temperature dependence of the stripe domain nucleation field and of the critical domain width. From these data we have deduced the thermal variation of both A and K_u up to 400 °C in an epi-

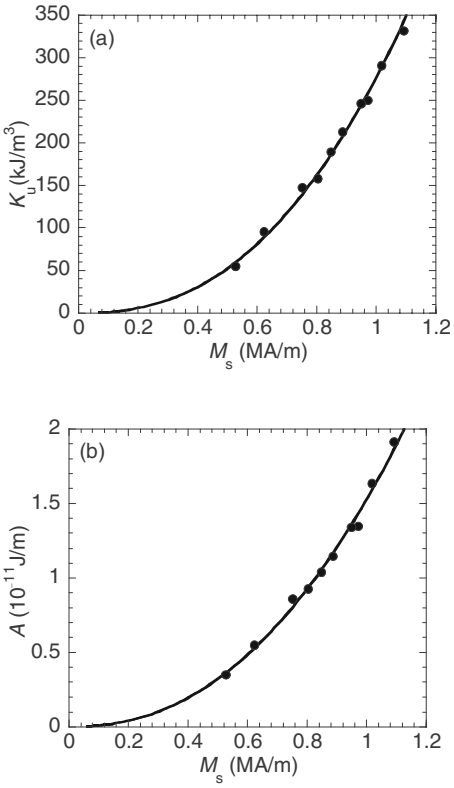

FIG. 11. Power fitting of the calculated values of (a) the uniaxial anisotropy constant and (b) the exchange stiffness constant as a function of the values of the saturation magnetization.

taxial, molecular beam epitaxy grown, FePd film, using literature data for the $M_s(T)$ dependence. Our approach does not depend on the particular method chosen to fully characterize the domain structure. Our findings for FePd films show that the ratio A/K_u is constant as temperature is varied and moreover that the thermal variation of both K_u and A compare reasonably well with M_s^2.

Our micromagnetic analysis was concerned with critical phenomena, a feature with several advantages. First of all, micromagnetic predictions can be expected to be far less sensitive to the role of defects and inhomogeneities, and furthermore are based on linearized equations, which can be analytically treated. Secondly, partly for the same reasons, the weak stripe domain theoretical analysis can be extended to the high temperature range, close to the Curie temperature.[26]

ACKNOWLEDGMENT

The present work has been supported by a FIRB Project of the Italian Ministry of Education and Research, entitled "Microsystems based on magnetic materials structured at the nanoscopic scale."

APPENDIX

From conditions (6) it follows that α, γ, $\tilde{\alpha}$, and $\tilde{\gamma}$ need to be real. Substituting m_x, m_y, and φ of expressions (7) into

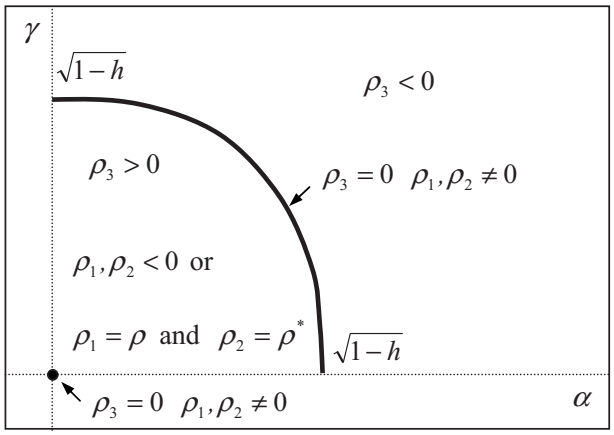

FIG. 12. Classification of the solutions of the bicubic equation with respect to reduced wave number values in the α-γ plane.

system (3) leads to an algebraic system of three equations which admits nonvanishing solutions if and only if the determinant of the coefficient matrix is vanishing. The obtained bicubic equation allows us to express the variable β^2 as a function of α^2 and γ^2. For each value of α^2 and γ^2 there are three corresponding roots ρ_1, ρ_2, and ρ_3 and so six values $\pm\beta_1$, $\pm\beta_2$, and $\pm\beta_3$ of β. Taking into account that the roots of the bicubic equation are continuous functions of α and γ, it follows that a root ρ_3 always exists positive in the first quadrant of the α-γ plane, inside the area between the axes and the circle of radius $\sqrt{1-h-\gamma^2}$, and vanishes at the origin and on the circle. The other two solutions ρ_1 and ρ_2 are real and negative inside the same area near the origin, but may become complex and conjugate approaching the circle. For $Q \to 0$ and $Q \to \infty$, the roots are all real and only for intermediate values of Q the bicubic equation may have complex and conjugate roots. Figure 12 summarizes the principal results of the above analysis.

As regards the region of space outside the film, substituting $\tilde{\varphi}$ in Eq. (4) allows us to find $\tilde{\beta}=-\sqrt{\tilde{\alpha}^2+\tilde{\gamma}^2}$ for $\eta > \delta/2$ and $\tilde{\beta}=\sqrt{\tilde{\alpha}^2+\tilde{\gamma}^2}$ for $\eta < \delta/2$.

Both the differential and the boundary condition equations (3)–(5) are linear and homogeneous. As a consequence, any linear combination of particular solutions with varying α, γ, $\beta=\pm\beta_j(\alpha^2,\gamma^2)$ $(j=1,2,3)$ $\tilde{\alpha}$, $\tilde{\gamma}$, is also a solution. Inserting the general linear combination inside the boundary conditions (5) we obtain $\tilde{\alpha}=\alpha$, $\tilde{\gamma}=\gamma$. Moreover, expressing the coefficients $B_j^{\pm}$ and $C_j^{\pm}$ as a function of $U_j^{\pm}$ through system (3), we get from Eqs. (5) an algebraic system of eight homogeneous equations in the eight unknown $U_j^{\pm}$, $\tilde{U}^{\pm}$. Next, we transform the above system into two separate systems of four equations in the four unknown $U_j=U_j^+-U_j^-$, $\tilde{U}=\tilde{U}^+-\tilde{U}^-$ and $U'=U_j^++U_j^-$, $\tilde{U}'=\tilde{U}^++\tilde{U}^-$. The two systems have different coefficient matrices. Consequently, if a system has nonvanishing solutions, the other one necessarily admits the trivial solution. Hence, we conclude that the solutions can be grouped into two symmetry classes. In the first class, the potential is an odd function of η. Hence, it follows that m_x is odd and m_y even. The second class is energetically disadvantaged because, being m_y an odd function of η, the surface

magnetic charge is an even function. The coefficient matrix determinant of the obtained system is a function of δ and h. The system has nonvanishing solutions only for particular values of δ and h and these values depend on α^2 and γ^2. We emphasize that for a given field h there are infinite δ solutions and the critical thickness which bears physical meaning is the minimum one. The above statement can be understood on the basis of energy considerations. It can be shown that the determinant of the algebraic system certainly vanishes for values of the reduced thickness δ within the interval $0 \leqslant \delta \leqslant 3\pi/\beta_3$. Moreover, along any line inside the circle quarter $\alpha=\sqrt{1-h-\gamma^2}$ that joins the origin of the α-γ plane with it, this solution presents surely a minimum. In particular, when $Q \rightarrow 0$ the problem can be solved analytically obtaining $\delta=\delta_c=2\pi/(1-h)$ and $D_c/W_c=\sqrt{(1+h)/(1-h)}$ for $\alpha=\sqrt{1-h^2}/2$ and $\gamma=0$[2]. Therefore, in the above limit, the critical thickness is always different from zero and takes the value $\delta_c=2\pi$ for zero external field. On the contrary, for strong anisotropy ($Q>1$) the critical thickness approaches zero when the field tends to the effective anisotropy field $h_A=1-1/Q$. The corresponding domain width grows up toward infinity ($\alpha=\gamma=0$).

Numerical calculations show that the critical thickness always corresponds to domains parallel to the external field ($\gamma=0$).[12,13] Moreover, they also show that outside the circle quarter $\alpha=\sqrt{1-h-\gamma^2}$ the coefficient matrix determinant of system (5) never vanishes.

*Present address: The Institute of Solid State Physics, The University of Tokyo, 5-1-5 Kashiwanoha, Kashiwa, Japan.

[1] A. Hubert and R. Schäfer, *Magnetic Domains*(Springer-Verlag, Berlin, 1998), p. 376.
[2] A. Hubert and R. Schäfer, *Magnetic Domains* (Springer-Verlag, Berlin, 1998), p. 390ff..
[3] P. E. Tannenwald and R. Weber, Phys. Rev. **121**, 715 (1961).
[4] R. Gemperle, E. V. Shtolts, and M. Zelený, Phys. Status Solidi **3**, 2015 (1963).
[5] A. P. Molozemoff and J. C. Slonczewski, *Magnetic Domain Walls in Bubble Materials* (Academic, New York, 1979), pp. 11–13.
[6] A. V. Ermakov and V. V. Maikov, Fiz. Met. Metalloved. **5**, 201 (1990).
[7] F. Bolzoni, F. Leccabue, R. Panizzieri, and L. Pareti, IEEE Trans. Magn. **20**, 1625 (1984).
[8] R. O'Handley, *Modern Magnetic Materials, Principles and Applications* (Wiley, New York, 2000), p. 511.
[9] T. Thomson, L. Abelmann, and P. Groenland, in *Magnetic Nanostructures in Modern Technology*, edited by B. Azzerboni, G. Asti, L. Pareti, and M. Ghidini, (Springer, Berlin, 2007).
[10] J. U. Thiele, S. Maat, J. L. Robertson, and E. E. Fullerton, IEEE Trans. Magn. **40**, 2537 (2004).
[11] A. Moser, K. Takano, D. T. Margulies, M. Albrecht, Y. Sonobe, Y. Ikeda, S. Sun, and E. E. Fullerton, J. Phys. D **35**, R157 (2002).
[12] M. W. Muller, Phys. Rev. **122**, 1485 (1961).
[13] W. F. Brown, Jr., Phys. Rev. **124**, 1348 (1961).
[14] V. Gehanno, A. Marty, B. Gilles, and Y. Samson, Phys. Rev. B **55**, 12552 (1997).
[15] H. A. Dürr, E. Dudzik, S. S. Dhesi, J. B. Goedkoop, G. van der Laan, M. Belakhovsky, C. Mocuta, A. Marty, and Y. Samson, Science **284**, 2166 (1999).
[16] J. B. Staunton, L. Szunyogh, A. Buruzs, B. L. Gyorffy, S. Ostanin, and L. Udvardi, Phys. Rev. B **75**, 144411 (2006).
[17] J. B. Staunton, S. Ostanin, S. S. A. Razee, B. L. Gyorffy, L. Szunyogh, B. Ginatempo, and Ezio Bruno, Phys. Rev. Lett. **93**, 257204 (2004).
[18] R. Pellicelli, Ph.D. thesis, Departement of Physics, University of Parma, 2007.
[19] G. Asti, M. Ghidini, R. Pellicelli, C. Pernechele, M. Solzi, F. Albertini, F. Casoli, S. Fabbrici, and L. Pareti, Phys. Rev. B **73**, 094406 (2006).
[20] Y. Samson, A. Marty, R. Hoffmann, V. Gehanno, and B. Gilles, J. Appl. Phys. **85**, 4604 (1999).
[21] M. Mulazzi, K. Chesnel, A. Marty, G. Asti, M. Ghidini, M. Solzi, M. Belakhovsky, N. Jaouen, J. M. Tonnerre and F. Sirotti, J. Magn. Magn. Mater. **272–276**, 895(E) (2004).
[22] E. Dudzik, S. S. Dhesi, H. A. Durr, S. P. Colling, M. D. Roper, G. van der Laan, K. Chesnel, M. Belakhovsky, A. Marty, and Y. Samson, Phys. Rev. B **62**, 5779 (2000).
[23] T. G. Phillips, Phys. Lett. **17**, 11 (1965).
[24] S. Okamoto, N. Kikuchi, O. Kitakami, T. Miyazaki, Y. Shimada, and K. Fukamichi, Phys. Rev. B **66**, 024413 (2002).
[25] K. D. Belashchenko, J. Magn. Magn. Mater. **270**, 413 (2004).
[26] N. Minnaja, Phys. Rev. B **1**, 1151 (1970).